

# Transcription is regulated by NusA:NusG interaction

Martin Strauß<sup>1</sup>, Christal Vitiello<sup>2</sup>, Kristian Schweimer<sup>1</sup>, Max Gottesman<sup>2,3</sup>, Paul Rösch<sup>1</sup> and Stefan H. Knauer<sup>1,\*</sup>

<sup>1</sup>Lehrstuhl Biopolymere und Forschungszentrum für Bio-Makromoleküle, Universität Bayreuth, 95447 Bayreuth, Germany, <sup>2</sup>Department of Microbiology and Immunology, Columbia University Medical Center, New York, NY 10032, USA and <sup>3</sup>Department of Biochemistry and Molecular Biophysics, Columbia University Medical Center, New York, NY 10032, USA

Received August 26, 2015; Revised May 04, 2016; Accepted May 05, 2016

## ABSTRACT

**NusA and NusG are major regulators of bacterial transcription elongation, which act either in concert or antagonistically. Both bind to RNA polymerase (RNAP), regulating pausing as well as intrinsic and Rho-dependent termination. Here, we demonstrate by nuclear magnetic resonance spectroscopy that the *Escherichia coli* NusG amino-terminal domain forms a complex with the acidic repeat domain 2 (AR2) of NusA. The interaction surface of either transcription factor overlaps with the respective binding site for RNAP. We show that NusA-AR2 is able to remove NusG from RNAP. Our *in vivo* and *in vitro* results suggest that interaction between NusA and NusG could play various regulatory roles during transcription, including recruitment of NusG to RNAP, resynchronization of transcription:translation coupling, and modulation of termination efficiency.**

## INTRODUCTION

Transcription, the first step in gene expression, is highly regulated by a multitude of transcription factors. The core transcription machinery is RNA polymerase (RNAP), which consists of five subunits in bacteria (2  $\times$   $\alpha$ ,  $\beta$ ,  $\beta'$ , and  $\omega$ ) (1). RNAP initiates RNA synthesis at a promoter (initiation), extends the nascent RNA (elongation), and releases the RNA at a terminator (termination) (2). Among *Escherichia coli* (*E. coli*) transcription factors, N-Utilization Substances (Nus) A and G are the only ones known to affect both the speed of RNA chain elongation and termination (3). NusG (Spt5 in archaea and eukaryotes), the only universally conserved transcription factor, is composed of an N-terminal domain (NTD) flexibly connected to a C-terminal domain (CTD) (Supplementary Figure S1A) (4,5). NusG-NTD interacts with the  $\beta'$  clamp helices ( $\beta'$ CH) and the  $\beta$  gate loop ( $\beta$ GL) of RNAP to increase RNAP processivity (4,6,7). NusG-CTD is target of at least two cellular

partners, termination factor Rho and antitermination factor NusE, which is identical to ribosomal protein S10 (8,9). NusA comprises an NTD that binds to the  $\beta$  flap tip helix of RNAP at the RNA exit channel, three RNA binding motifs (S1, KH1, KH2) that together form the SKK domain, and, in *E. coli* and other  $\gamma$ -proteobacteria, two additional C-terminal acidic repeat domains (AR1, AR2; Supplementary Figure S1B) (10–14). NusA-AR1 interacts with N protein of phage  $\lambda$ , but is not essential for N-mediated suppression of transcription termination (antitermination) (15–17). NusA-AR2 can bind either to the CTD of the RNAP  $\alpha$ -subunit ( $\alpha$ CTD) or to the NusA-SKK. NusA-AR2 attached to NusA-SKK autoinhibits NusA activity by preventing RNA binding (15,18).

NusA and NusG differentially alter the properties of the transcription elongation complex (TEC) *via* direct and independent interactions (3). NusG increases TEC processivity whereas NusA slows RNAP by either increasing pause times or by introducing new pause sites (19). The two factors have context-dependent effects on termination and act either in concert or as antagonists. On the one hand, NusG and NusA are proposed to support Rho cooperatively to suppress the toxic functions of foreign genes. On the other hand, both are part of antitermination complexes on ribosomal RNA and phage  $\lambda$  nascent transcripts (20–23). Furthermore, NusA can enhance or decrease both Rho-dependent and intrinsic termination efficiency, depending on the specific terminator (reviewed in (24,25)). NusG, in contrast, enhances termination exclusively at Rho-dependent sites (26,27). Importantly, NusG serves as the physical linker between the RNAP and the ribosome by binding RNAP *via* NusG-NTD and S10 *via* NusG-CTD, thus coupling transcription and translation (8).

NusA and NusG bind to different sites on RNAP (6,7,10). Although these sites are in close proximity, a direct connection between the two factors has not been reported thus far. With nuclear magnetic resonance (NMR) spectroscopy we here demonstrate that NusA and NusG do

\*To whom correspondence should be addressed. Tel: +49 921 553868; Fax: +49 921 16490459; Email: stefan.knauer@uni-bayreuth.de  
Present address: Martin Strauß, Department of Microbiology and Immunology, Columbia University Medical Center, New York, NY 10032, USA.

specifically mutually interact and, supported by *in vivo* and *in vitro* data, we propose that this interaction may have key regulatory roles in diverse steps of transcription.

## MATERIALS AND METHODS

### Cloning

*nusA* was cloned into the pTKK19 expression vector (28) via NdeI and BamHI restriction sites resulting in the recombinant plasmid pTKK19\_nusA(1-495). The recombinant protein carried a deca-histidine tag followed by a PreScission cleavage site at its N-terminus.

### Gene expression and protein purification

Gene expression and protein purification procedures for NusG, NusG-NTD, NusG-CTD, NusA-NTD, NusA-SKK, NusA-AR1 and  $\alpha$ CTD were described earlier (8,16,29–32). NusA-AR2 (NusA(424–495)) was produced as fusion protein with His<sub>10</sub> tag followed by PreScission protease cleavage site at its N-terminus. Its gene expression and protein purification were according to the protocol for NusA(339–495) (33). His<sub>10</sub>-NusA-AR2 was purified like NusA-AR2 omitting the tag-removal step.

*nusA* was expressed in *E. coli* BL21 (DE3) harboring pTKK19\_nusA(1-495). Cells were grown in lysogeny broth (LB) medium containing 30  $\mu$ g/ml kanamycin at 37°C. At an optical density at 600 nm (*OD*<sub>600</sub>) of  $\sim$ 0.7 expression was induced by 1 mM isopropylthiogalactoside (IPTG). Cells were harvested after 4 h (9,000  $\times$  g, 15 min, 4°C), resuspended in buffer A (20 mM Tris(hydroxymethyl)aminomethane (Tris)/HCl, pH 7.9, 500 mM NaCl, 5 mM imidazole, 1 mM  $\beta$ -mercaptoethanol) and disrupted by a microfluidizer (Microfluidics, Newton, MA, USA). After centrifugation (12,000  $\times$  g, 30 min, 4°C) the crude extract was applied to a 5 ml HisTrap HP column (GE Healthcare, Munich, Germany) and eluted using a step gradient from 5 mM to 1 M imidazole in buffer A. Fractions containing the His<sub>10</sub>-NusA fusion protein were combined and the protein was cleaved by PreScission protease during dialysis against buffer B (20 mM Tris/HCl, pH 8, 1 mM  $\beta$ -mercaptoethanol) at 4°C overnight. The protein solution was applied to a 5 ml GStrap FF column (GE Healthcare, Munich, Germany) and the flow-through subsequently to a 5 ml QXL column (GE Healthcare, Munich, Germany). NusA was eluted using a step gradient from 0 to 1 M NaCl in buffer B. Fractions containing pure NusA were combined, dialyzed against 5 l 20 mM Tris/HCl, pH 7.5, 50 mM NaCl, 1 mM dithiothreitol (DTT), concentrated using ultrafiltration units (Viva Science, molecular weight cut-off (MWCO): 10 kDa), shock frozen in liquid nitrogen, and stored at  $-80^\circ\text{C}$ .

Production and purification of RNAP for NMR experiments was based on Ref. (34). In brief, *E. coli* BL21(DE3) (Novagen, Madison, WI, USA) harboring a plasmid containing *rpoA*, *rpoB*, *rpoC* and *rpoZ* in one operon under control of T7 promoter was used for gene expression. The  $\beta'$  subunit was produced as fusion protein carrying a His<sub>6</sub> tag at its C-terminus. 2 l of LB medium in a 5 l flask supplemented with 100  $\mu$ g/ml ampicillin were inoculated with an overnight culture to an *OD*<sub>600</sub> of 0.02 and incubated at

37°C and 150 rpm. Having reached an *OD*<sub>600</sub> of 0.2 the temperature was decreased to 20°C. After 2 h, IPTG was added to a final concentration of 0.5 mM for induction, and the culture was incubated overnight. Cells were then harvested by centrifugation for 15 min at 4°C and 9,000  $\times$  g, resuspended in buffer C (50 mM Tris/HCl, pH 6.9, 0.5 M NaCl, 5 % (v/v) glycerol, 1 mM DTT) and lysed with a microfluidizer (Microfluidics, Newton, MA, USA). RNAP was purified by nickel affinity chromatography with 2  $\times$  5 ml Ni<sup>2+</sup>-nitrilotriacetic acid (NTA) Superflow columns (QIAGEN) and eluted by a constant gradient from 0 to 1 M imidazole in buffer C. Peak fractions containing RNAP were dialyzed against buffer D (50 mM Tris/HCl, pH 6.9, 0.5 mM ethylenediaminetetraacetic acid (EDTA), 5 % (v/v) glycerol, 1 mM DTT) overnight at 4°C and then applied to a 5 ml Heparin HP column (GE Healthcare), followed by elution with a constant NaCl gradient from 0 to 1 M NaCl in buffer D. Fractions containing RNAP were pooled, dialyzed against buffer B overnight at 4°C, applied to a 25 ml Q-Sepharose FF column, and eluted with a constant gradient from 0 to 1 M NaCl in buffer B. RNAP containing fractions were concentrated using ultrafiltration units (Viva Science, MWCO: 10 kDa), shock frozen in liquid nitrogen, and stored at  $-80^\circ\text{C}$ .

Production and purification of RNAP for *in vitro* transcription assays was carried out as described (35), with minor modifications.

### Isotopic labeling of proteins

Proteins were uniformly labeled with <sup>15</sup>N or <sup>15</sup>N,<sup>13</sup>C by growing *E. coli* in M9 minimal medium (36,37) supplemented with (<sup>15</sup>NH<sub>4</sub>)<sub>2</sub>SO<sub>4</sub> (Campro Scientific, Berlin, Germany) or (<sup>15</sup>NH<sub>4</sub>)<sub>2</sub>SO<sub>4</sub> and <sup>13</sup>C-D-glucose (Cambridge Isotope laboratories, Inc., Andover, MA, USA) as the only nitrogen and carbon source, respectively. Expression and purification procedures were identical to those used for proteins produced in LB medium.

### Pull-down assay

The pull-down assay was performed with a 1 ml HisTrap HP column (GE Healthcare) equilibrated with buffer E (10 mM potassium phosphate, pH 6.9, 50 mM NaCl). The proteins were dialyzed against buffer E overnight at 4°C before application to the column. The application volume was always 1 ml. After extensive washing with buffer E, elution was carried out with 100 or 400 mM imidazole in buffer E, respectively, and resulted in a mixture of His<sub>10</sub>-NusA-AR2 and NusG-NTD (400  $\mu$ M and 200  $\mu$ M, molar ratio: 2:1) as assayed, with His<sub>10</sub>-NusA-AR2 (200  $\mu$ M) alone and NusG-NTD (400  $\mu$ M) alone as controls.

### *In vitro* transcription assay

RNA and DNA oligonucleotides were commercially synthesized by Integrated DNA Technologies with sequences derived from the T7A1 promoter sequence. Assembly of the TEC and the *in vitro* transcription were carried out as described (38). Briefly, a 65mer template DNA strand was hybridized to an 11mer RNA labeled with <sup>32</sup>P at the 5'

end. 50 pmol RNAP in transcription buffer (TB, 20 mM Tris/HCl, pH 7.9, 5 mM MgCl<sub>2</sub>, 40 mM KCl, 2 mM β-mercaptoethanol) were mixed with equimolar concentrations of the DNA:RNA hybrid, followed by addition of the nontemplate DNA strand. The assembled TECs were purified by affinity chromatography using Ni<sup>2+</sup>-nitrilotriacetic acid agarose (QIAGEN) and subsequent membrane filtration with Ultrafree<sup>®</sup> 0.65 μm PVDF centrifugal filters (Millipore). 2.5 μM TEC were incubated with 50 μM of one or both transcription factors or TB for 10 min at 25°C. When two proteins were tested they were added simultaneously, as previous tests indicated that the order of addition had no effect. Transcription was initiated by addition of 1 mM NTPs and stopped after 60 seconds by addition of an equal volume of 2x loading buffer (10M urea, 50 mM EDTA, pH 7.9, 0.05 % (w/v) bromophenol blue, and 0.05 % (w/v) xylene cyanol). RNA products were resolved on a 23 % denaturing polyacrylamide gel containing 7 M urea. Gels were exposed to phosphor screens and scanned by Typhoon Phosphorimager (GE Healthcare Life Sciences).

### NMR experiments

All NMR spectra were recorded at 298 K on Bruker Avance 700 MHz and Avance 800 MHz spectrometers with cryogenically cooled triple-resonance probes equipped with pulsed field-gradient capabilities. Processing of NMR data was carried out using in-house routines and visualized by NMRView (39). For all NMR experiments the proteins were in 10 mM potassium phosphate buffer, pH 6.4, 50 mM NaCl, at 298 K. The initial sample volume was 550 μl if not stated otherwise. Backbone assignments of NusG-NTD, NusG-CTD, NusA-AR2, and αCTD were taken from previous studies (4,18,32).

To evaluate [<sup>1</sup>H,<sup>15</sup>N]-heteronuclear single quantum coherence (HSQC) titration experiments we calculated the normalized chemical shift changes ( $\Delta\delta_{\text{norm}}$ ) according to Equation (1).

$$\Delta\delta_{\text{norm}} = \sqrt{\Delta\delta(^1\text{H})^2 + [0.1 \cdot \Delta\delta(^{15}\text{N})]^2} \quad (1)$$

Dissociation constants ( $K_D$ ) were calculated from [<sup>1</sup>H,<sup>15</sup>N]-HSQC titrations by analyzing the chemical shift changes and fitting a two-state model as in Equation (2) to the chemical shift change of amide protons showing fast exchange on the chemical shift timescale.

$$\Delta\nu = \Delta\nu_{\text{End}} \cdot \frac{[P]_0 \cdot r + [P]_0 + K_D - \sqrt{(K_D + [P]_0 + [P]_0 \cdot r)^2 - 4 \cdot ([P]_0)^2 \cdot r}}{2 \cdot [P]_0} \quad (2)$$

where  $\Delta\nu$  is the normalized resonance frequency difference in Hz,  $\Delta\nu_{\text{End}}$  the normalized resonance frequency difference between free and fully bound protein in Hz,  $K_D$  the dissociation constant,  $r$  the protein:labeled protein ratio and  $[P]_0$  the total concentration of <sup>15</sup>N-labeled protein.  $K_D$  and  $\Delta\nu_{\text{End}}$  were used as fitting parameters. The reduction of  $[P]_0$  due to dilution was accounted for during fitting.

For the displacement experiment of <sup>15</sup>N-NusA-AR2 from αCTD by NusG-NTD separate samples were prepared for <sup>15</sup>N-NusA-AR2 (100 μM, 500 μl) and <sup>15</sup>N-NusA-AR2: αCTD (100 μM each, 500 μl). NusG-NTD was then added to the latter sample from a 287 μM stock solution.

For the quantitative analysis of signal intensities in the displacement experiments signal intensities were normalized by the number of scans, the concentration, and the length of the 90° proton pulse.

### Docking

The complex of NusA-AR2 and NusG-NTD was modeled with the HADDOCK webserver (40) using data from the [<sup>1</sup>H,<sup>15</sup>N]-HSQC titrations as restraints (active residues in NusG-NTD: 4, 13, 15, 18, 44, 50, 51, 52, 58, 59, 61, 95, 104, 105, 106, 107, 109, 114, 117 and 118; active residues in NusA-AR2: 463, 474, 483, 487, 489, 490, 491 and 493). Passive residues were determined automatically. The NMR ensembles of NusA-AR2 (Protein Data Bank (PDB) ID: 1WCN) and NusG-NTD (PDB ID: 2K06) were used as input.

### Strains and β-galactosidase assays

Strains were derivatives of MDS42, which lacks prophages and insertion elements (41) containing λ fusions (42). *lacZ* is expressed from the fusions  $\lambda cI857 - pR - cro(\Delta RBS) - nutR - tRI - cII::lacZ$  or  $\lambda cI857 - pR - cro_{27} - nutR - tRI - cII::lacZ$ . The TAAGGAGGTTGT to TacctccTTGT substitution in the *cro* ribosome binding site (RBS), blocks *cro* translation in the former strain (*cro*( $\Delta RBS$ )). *cro*<sub>27</sub> has an RBS, but *Cro*<sub>27</sub> is non functional due to an amino acid exchange (R27Q). The creation of strains 10323 and 10881 was described previously (18). The *rhoE134K* mutation was introduced by phage P1 transduction, resulting in a Rho variant which is non functional at  $\lambda tRI$ . The strains carrying *nusA* variants were constructed by recombineering.

Cells were assayed for β-galactosidase activity (Miller units) after overnight growth at 37°C. β-galactosidase activity of cells with defective Rho (*rho15*) was set to 100 % (strains 11633 and 11634), since termination was completely abolished at  $\lambda tRI$ . Assays were performed independently four times and resulting activities were averaged.

### Programmes

Graphical representations of protein structures were created with PyMOL (43). Sequence alignments were done with Clustal omega (44).

## RESULTS AND DISCUSSION

### NusG interacts specifically with NusA

First, we probed a possible NusA:NusG interaction by NMR spectroscopy with full-length proteins. Addition of NusA to <sup>15</sup>N-labeled NusG to equimolar concentration resulted in a strong decrease of NusG-NTD signals in the [<sup>1</sup>H,<sup>15</sup>N]-HSQC spectrum, whereas NusG-CTD signals were weakened only marginally (Figure 1A). The high transversal relaxation rate of the 54.9 kDa NusA strongly affects magnetization transfer efficiency upon binding, which leads to line broadening and ultimately to a decrease of signal intensity. Thus, the observed loss of NusG-NTD signals suggests direct NusA:NusG-NTD interaction. Specific NusA:NusG-NTD complex formation was confirmed



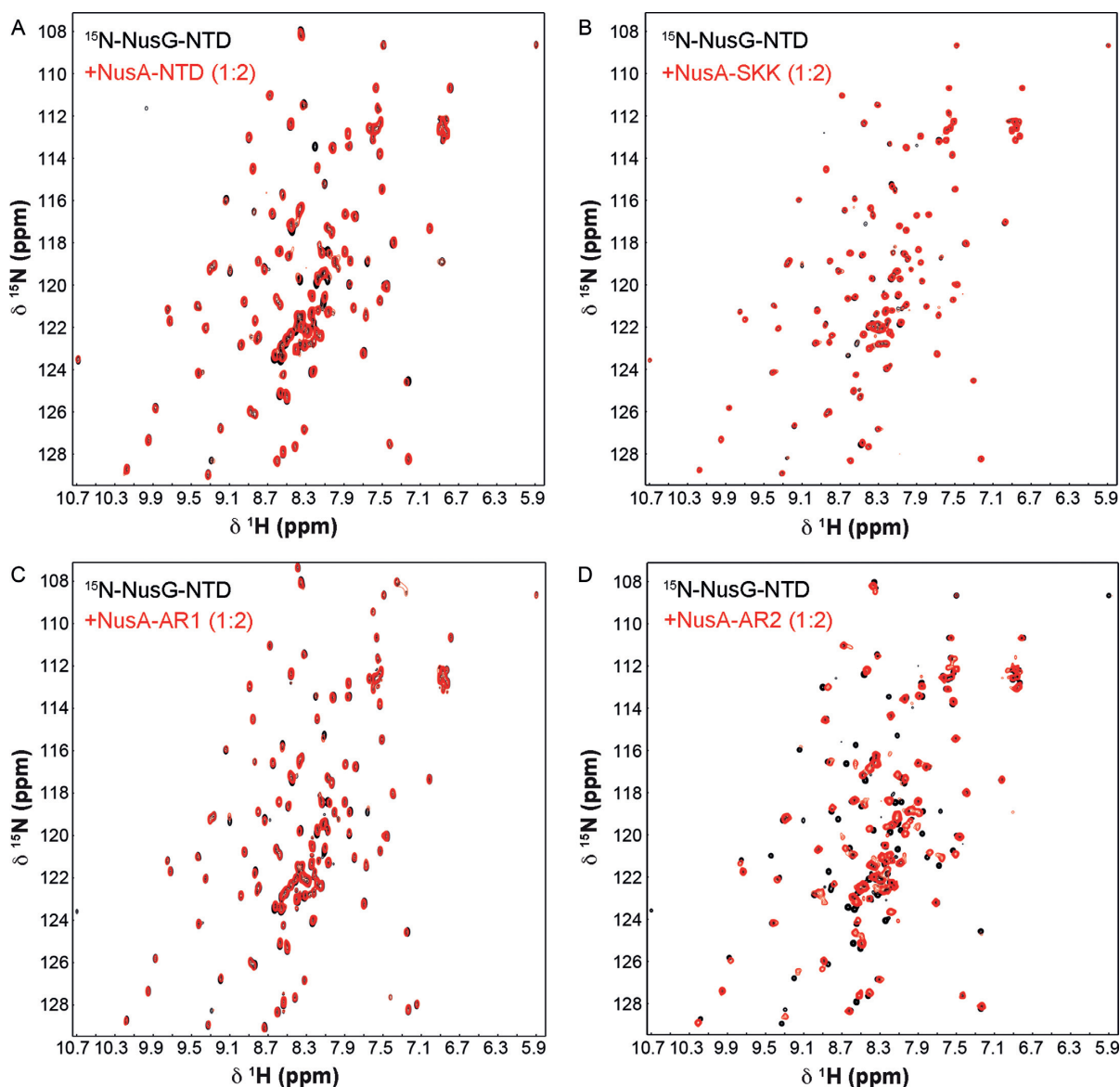


**Figure 2.** NusG-NTD interacts with NusA-AR2.  $[^1\text{H}, ^{15}\text{N}]$ -HSQC spectra of  $^{15}\text{N}$ -NusG-NTD in the absence, black, or presence, red, of (A) NusA-NTD, (B) NusA-SKK, (C) NusA-AR1, and (D) NusA-AR2.  $^{15}\text{N}$ -NusG-NTD was present at 100  $\mu\text{M}$  in all experiments, and NusA domains were added in a twofold molar excess.

to a final three-fold molar excess of NusG-NTD partially reversed these shifts, indicating that NusG-NTD can displace NusA-AR2 from the  $\alpha\text{CTD}$ . Although the displacement was incomplete due to the lower  $K_D$  of NusA-AR2: $\alpha\text{CTD}$  ( $K_D < 5 \mu\text{M}$ ) (18) versus NusA-AR2:NusG-NTD ( $K_D$ : 24  $\mu\text{M}$ ), it confirms that the RNAP/NusA-AR2 binding sites on NusG-NTD overlap as do the  $\alpha\text{CTD}$ /NusG-NTD interaction interfaces on NusA-AR2. This finding was counter-checked by the displacement of  $^{15}\text{N}$ -NusA-AR2 from  $\alpha\text{CTD}$  by NusG-NTD (Supplementary Figure S7). Addition of  $\alpha\text{CTD}$  to  $^{15}\text{N}$ -NusA-AR2 to equimolar concentration resulted in chemical shift changes of signals from  $^{15}\text{N}$ -NusA-AR2 typical for  $^{15}\text{N}$ -NusA-AR2: $\alpha\text{CTD}$  complex formation (18). Subsequent addition of NusG-NTD caused the  $^{15}\text{N}$ -NusA-AR2 signals to shift towards the resonance positions of the  $^{15}\text{N}$ -NusA-AR2:NusG-NTD

complex. Again, the displacement was incomplete owing to the difference in the affinities of NusA-AR2 to  $\alpha\text{CTD}$  and NusG-NTD.

We extended these studies to full-length proteins step-by-step. In an initial experiment we added RNAP to  $^{15}\text{N}$ -NusG, which led to a loss of almost all  $^{15}\text{N}$ -NusG signals in the  $[^1\text{H}, ^{15}\text{N}]$ -HSQC spectrum owing to the dramatic increase of the NusG rotational correlation time upon formation of the NusG:RNAP complex (Supplementary Figure S8A). Although NusG-NTD is only flexibly linked to NusG-CTD and NusG is supposed to interact with RNAP *via* NusG-NTD (4), NusG-CTD signals were not observable in the  $^{15}\text{N}$ -NusG:RNAP complex. Thus, either NusG-CTD is sterically hindered in the complex so that it cannot move freely, or NusG-CTD interacts directly with RNAP. To exclude such direct NusG-CTD:RNAP interac-

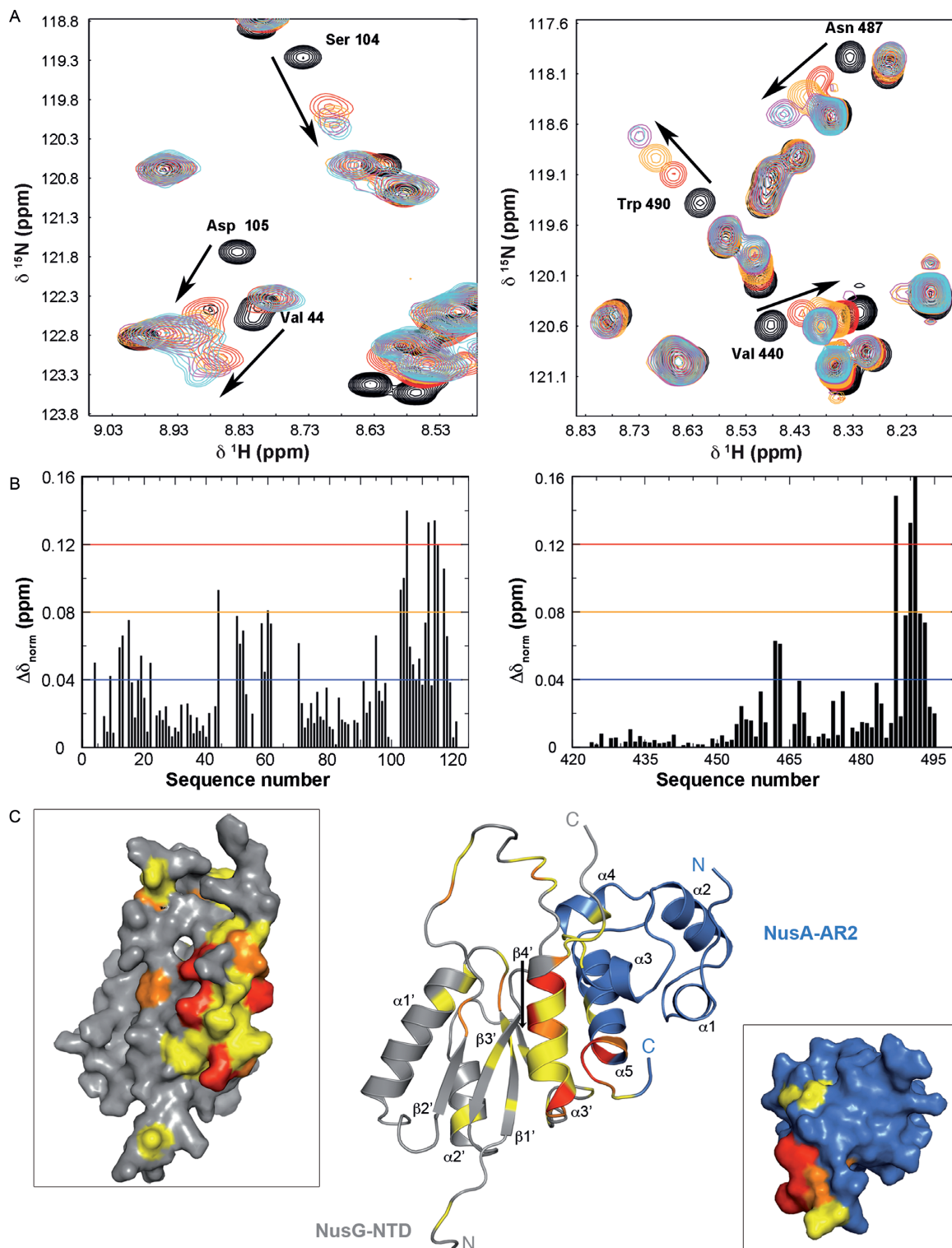


**Figure 3.** NusG-NTD:NusA-AR2 complex formation. (A, left) Sections of the  $[\text{}^1\text{H}, \text{}^{15}\text{N}]$ -HSQC-spectra of the titration of  $140\ \mu\text{M}$   $^{15}\text{N}$ -NusG-NTD with NusA-AR2. NusA-AR2 was added in a molar ratio of 1:0, black, 1:0.75, red, 1:1.25, orange, 1:2.5, magenta, and 1:3.5, cyan (stock concentration of NusA-AR2: 1.1 mM). (right) Sections of the  $[\text{}^1\text{H}, \text{}^{15}\text{N}]$ -HSQC-spectra of the titration of  $100\ \mu\text{M}$   $^{15}\text{N}$ -NusA-AR2 with NusG-NTD. Spectra corresponding to molar ratios 1:0, 1:0.5, 1:1, 1:2.5, and 1:3 are in black, red, orange, magenta, and cyan, respectively (stock concentration of NusG-NTD:  $300\ \mu\text{M}$ ). Arrows indicate chemical shift changes during the titrations, selected signals are assigned. (B) HSQC-derived normalized chemical shift changes versus sequence position. (left)  $\Delta\delta_{\text{norm}}$  of  $^{15}\text{N}$ -NusG-NTD on titration with NusA-AR2; (right)  $\Delta\delta_{\text{norm}}$  of  $^{15}\text{N}$ -NusA-AR2 on titration with NusG-NTD. Horizontal lines: significance levels of  $\Delta\delta_{\text{norm}}$  (ppm) = 0.12, red; = 0.08, orange; = 0.04, blue. (C) Model of the NusA-AR2:NusG-NTD complex. The complex was generated with HADDOCK using the chemical shift perturbations of the  $[\text{}^1\text{H}, \text{}^{15}\text{N}]$ -HSQC titrations as restraints. The model with the best HADDOCK score is depicted. NusA-AR2 (PDB ID: 2K06), blue, and NusG-NTD (PDB ID: 1WCN), grey, are in cartoon representation. The normalized chemical shift changes from (B) are mapped on the structures ( $0.04\ \text{ppm} < \Delta\delta_{\text{norm}} < 0.08\ \text{ppm}$ , yellow;  $0.08\ \text{ppm} < \Delta\delta_{\text{norm}} < 0.12\ \text{ppm}$ , orange;  $\Delta\delta_{\text{norm}} > 0.12\ \text{ppm}$ , red). Panels show the surface representations of NusG-NTD, left, and NusA-AR2, right.

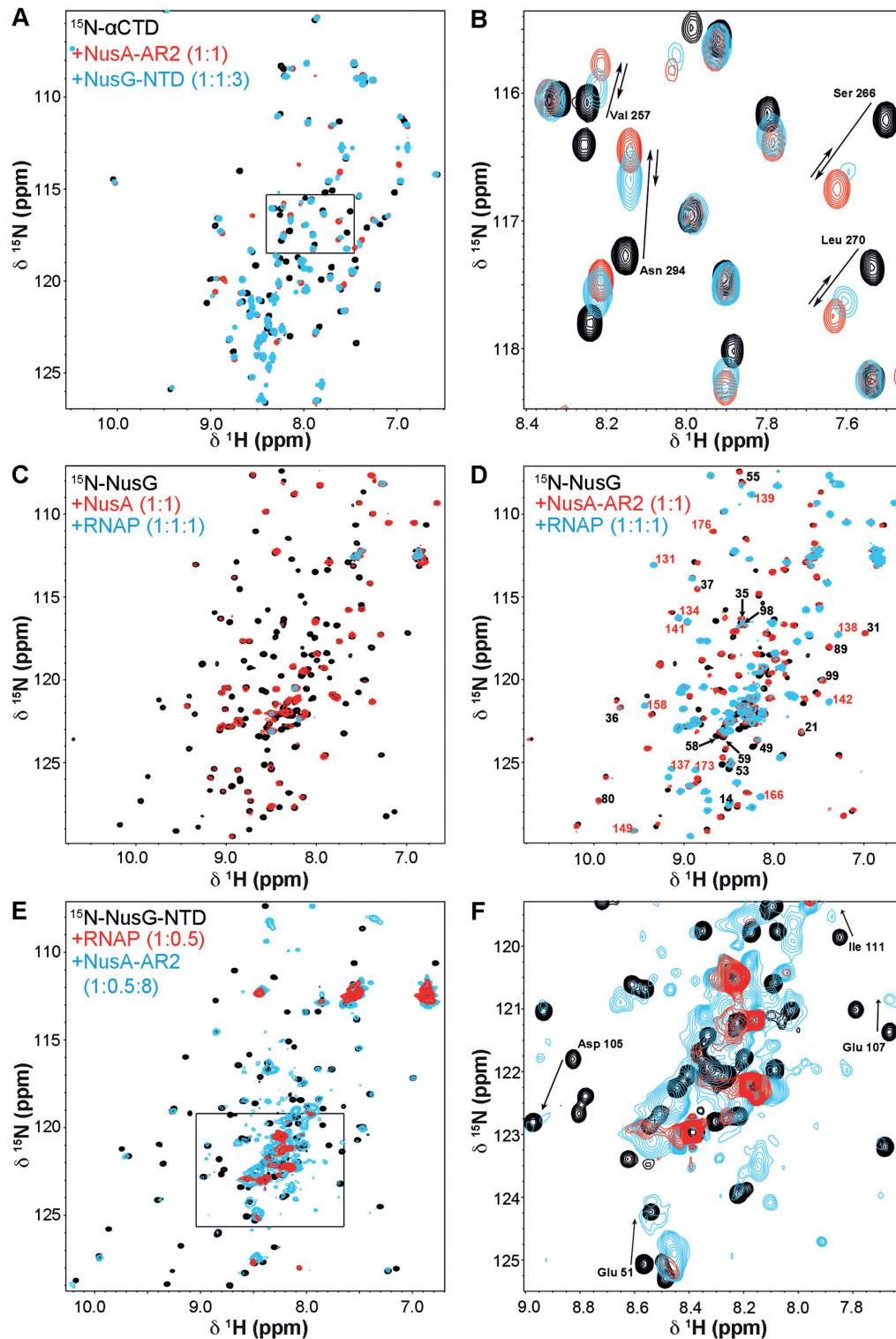


**Figure 4.** NusG-NTD:NusA-AR2 interaction in the presence of RNAP. (A and B)  $^1\text{H}$ ,  $^{15}\text{N}$ -HSQC displacement experiment of NusA-AR2 from  $^{15}\text{N}$ - $\alpha\text{CTD}$  by NusG-NTD. Black,  $^{15}\text{N}$ - $\alpha\text{CTD}$ ; red,  $^{15}\text{N}$ - $\alpha\text{CTD}$ :NusA-AR2 = 1:1; blue,  $^{15}\text{N}$ - $\alpha\text{CTD}$ :NusA-AR2:NusG-NTD = 1:1:3. The concentration of  $^{15}\text{N}$ - $\alpha\text{CTD}$  was always  $50\ \mu\text{M}$ . The rectangle in (A) indicates the section as in (B). The arrows in (B) show the changes in the chemical shifts of selected residues. (C) NusG binds to NusA in the presence of RNAP.  $^1\text{H}$ ,  $^{15}\text{N}$ -HSQC spectra of  $^{15}\text{N}$ -NusG, black,  $^{15}\text{N}$ -NusG in the presence of NusA (molar ratio 1:1), red, and  $^{15}\text{N}$ -NusG in the presence of NusA and RNAP (molar ratio 1:1:1), cyan. (D) NusG binds to NusA-AR2 in the presence of RNAP.  $^1\text{H}$ ,  $^{15}\text{N}$ -HSQC spectra of  $^{15}\text{N}$ -NusG, black,  $^{15}\text{N}$ -NusG in the presence of NusA-AR2 (molar ratio 1:1), red, and  $^{15}\text{N}$ -NusG in the presence of NusA-AR2 and RNAP (molar ratio 1:1:1), cyan. Selected signals are labeled (black, NusG-NTD signals; red, NusG-CTD signals). The concentration of  $^{15}\text{N}$ -NusG was  $50\ \mu\text{M}$  in all experiments in (C) and (D). (E) NusA-AR2 removes NusG-NTD from RNAP.  $^1\text{H}$ ,  $^{15}\text{N}$ -HSQC spectra of  $^{15}\text{N}$ -NusG-NTD, black,  $^{15}\text{N}$ -NusG-NTD in the presence of RNAP (molar ratio 1:0.5), red, and  $^{15}\text{N}$ -NusG-NTD in the presence of RNAP and NusA-AR2 (molar ratio 1:0.5:8), cyan. The concentration of  $^{15}\text{N}$ -NusG was always  $50\ \mu\text{M}$ . The rectangle in (E) indicates the section as in (F). In (F), selected signals are assigned with arrows indicating changes in their chemical shifts corresponding to the complex formation of  $^{15}\text{N}$ -NusG-NTD and NusA-AR2.

tion, we monitored isolated  $^{15}\text{N}$ -NusG-CTD in the presence of RNAP in a separate experiment and found no changes in the  $[^1\text{H}, ^{15}\text{N}]$ -HSQC spectra as compared to  $^{15}\text{N}$ -NusG-CTD alone (Supplementary Figure S8B). Consequently, the loss of all  $^{15}\text{N}$ -NusG signals upon RNAP addition solely originates from formation of the NusG-NTD:RNAP complex.

To probe the NusA:NusG interaction in the presence of full-length RNAP we added NusA to  $^{15}\text{N}$ -NusG, leaving only NusG-CTD signals visible (Figure 4C and Supplementary Figure S8C). On addition of RNAP all signals decreased (Figure 4C and Supplementary Figure S8C). Thus, either (i) NusA:NusG interaction is disrupted by RNAP and both NusA and NusG bind individually to RNAP, or (ii) NusA:NusG remains intact and interacts with RNAP *via* NusA-NTD, or (iii) both. To eliminate interference by NusA-NTD:RNAP interactions, we repeated the experiment using isolated NusA-AR2 instead of full-length NusA (Figure 4D and Supplementary Figure S8D). When NusA-AR2 was present, the  $[^1\text{H}, ^{15}\text{N}]$ -HSQC spectrum of  $^{15}\text{N}$ -NusG showed chemical shift changes corresponding to NusG-NTD:NusA-AR2 complex formation (see also Figure 2D). On addition of RNAP the intensity of the NusG signals decreased, however, in contrast to the experiment with full-length NusA, both NusG-NTD and NusG-CTD signals remained visible with the chemical shifts of the NusG-NTD:NusA-AR2 complex. We conclude (i) that at least some of the NusG-NTD:NusA-AR2 complexes remain intact in the presence of RNAP and (ii) that these complexes cannot bind to RNAP in the absence of NusA-NTD. This confirms that NusA-AR2:NusG and NusG:RNAP formation are mutually exclusive. The decrease in signal intensity may be explained by dissociation of a certain portion of the NusG-NTD:NusA-AR2 complex so that NusG binds to RNAP, and NusA-AR2 either interacts with the  $\alpha$ CTD of RNAP or remains free. Thus, with full length NusA, the NusG:NusA complex is stable and is connected to RNAP *via* NusA-NTD, although a fraction of NusG and NusA might interact with RNAP individually.

We next demonstrated that NusA-AR2 can remove NusG-NTD from RNAP (Figure 4E). As expected,  $^{15}\text{N}$ -NusG-NTD signals were drastically diminished by addition of RNAP. However, they reappeared upon NusA-AR2 addition with the chemical shift perturbations typical for the NusG-NTD:NusA-AR2 complex. Hence, NusA-AR2 and RNAP compete for NusG-NTD.

### NusA-AR2 induces pausing and blocks NusG suppression of pausing *in vitro*

We then asked if the NusA-AR2:NusG-NTD interaction affects transcription *in vitro*. For this we utilized a nucleic acid scaffold to generate a transcription elongation complex (TEC) which carries an 11 nt  $^{32}\text{P}$ -labeled RNA primer base-paired to template DNA and flanked by non-template DNA (TEC11A, for details see Materials and Methods). Transcription was initiated by the addition of the four NTPs and stopped after 60 seconds. The TEC paused at several intrinsic pause sites in the template in the absence of additional transcription factors, with pause 1 being the most prominent (Figure 5; lane 2). Full-length NusG suppressed pause

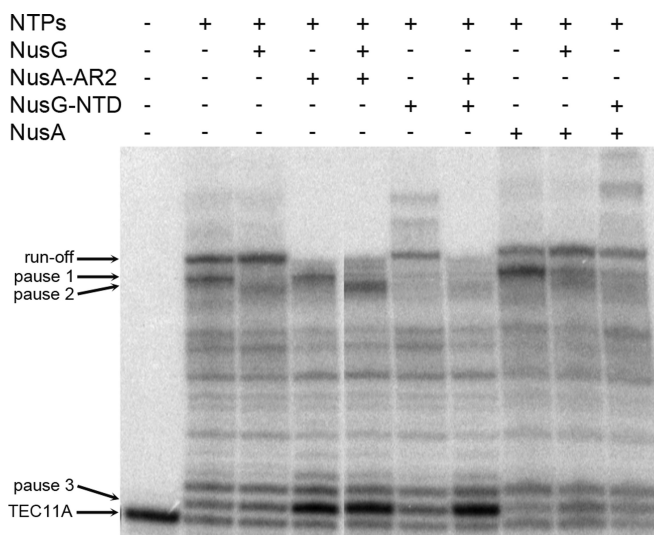


**Figure 5.** *In vitro* transcription assay for combinations of NusG, NusA, NusG-NTD and NusA-AR2. 23 % urea-polyacrylamide gel. The assembled TEC (TEC11A) was pre-incubated with NusG, NusA, NusA-AR2, NusG-NTD, combinations of these, or transcription buffer for 10 min at 25°C. Transcription was started by NTP addition and stopped after 60 s. TEC11A, run-off, and three pause sites are indicated by arrows.

1, increased run-off transcription and introduced a weak new pause, pause 2 (lane 3). NusA-AR2, interestingly, generated a strong pause at position 12C (pause 3), 1 nt downstream of the transcription start site, without influencing other pause sites (lane 4). Moreover, NusA-AR2 completely blocked run-off transcription (lane 4). When both proteins were present in equimolar amounts, pause 2 was enhanced, whereas pause 1 and run-off transcripts were suppressed (lane 5). Enhancement of NusG-dependent pause 2 is consistent with an interaction between NusG and NusA-AR2, possibly explained by the inability of NusG-NTD to enhance processivity when bound to NusA-AR2. The NusA-AR2-dependent pause 3 was not influenced by NusG (lane 5). NusG-NTD yielded similar results as full-length NusG. It suppressed pause 1 (lane 6), and this suppression was abrogated by NusA-AR2 (lane 7). As with full-length NusG, NusG-NTD did not affect NusA-AR2-induced pause 3 (lane 7).

Full-length NusA enhanced pause 1, but did not, however, induce pausing at pause 3 (lane 8). This suggests that the NusA-AR2 domain in full-length NusA was still bound to the NusA-SKK domain, and was not free to interact with the initiating TEC. Unlike NusA-AR2, suppression of pause 1 by full-length NusG or NusG-NTD was not completely abrogated by full-length NusA, possibly because NusA-AR2 remains bound to the NusA-SKK domain during elongation, and is not available to interact with NusG-NTD (lanes 8–10).

The ability of isolated NusA-AR2 to pause the TEC at 12C (pause 3) was unexpected. It suggests that at least early in elongation, when RNA has not yet extruded from the exit channel, NusA-AR2 may still be bound to the SKK domain and may thus be unavailable to interact with  $\alpha$ CTD. In addition, the ability of NusA-AR2 to induce a strong pause

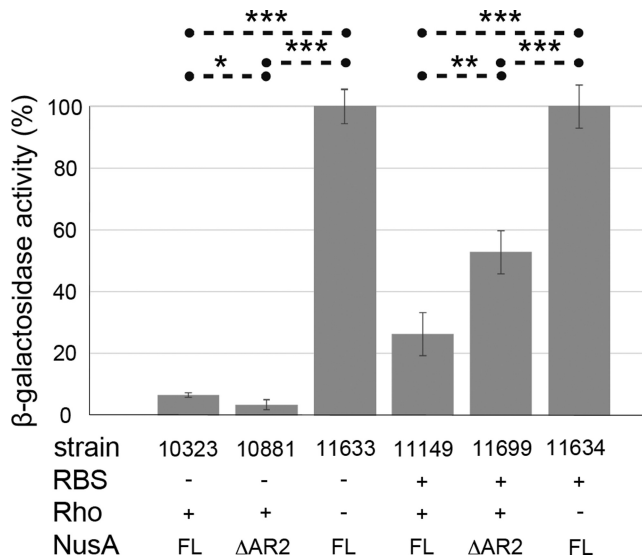


**Figure 6.** Deletion of NusA-AR2 affects termination at  $\lambda tR1$ .  $\beta$ -galactosidase reporter assays were performed with *lacZ* fusions  $\lambda cI857 - pR - cro(\Delta RBS) - nutR - tR1 - cII::lacZ$  and  $\lambda cI857 - pR - cro27 - nutR - tR1 - cII::lacZ$ . Strains are derivatives of *E. coli* MDS42. Cells were assayed for  $\beta$ -galactosidase activity (Miller units) after overnight growth at 37°C.  $\beta$ -galactosidase activity of cells with defective Rho was set to 100% (strains 11633 and 11634). *P* values are < 0.05 (\*), < 0.01 (\*\*), or < 0.001 (\*\*\*). RBS +/-, functional/defective RBS; Rho +/-, functional/defective Rho; FL, full length.

implies that NusA-AR2 might act as a regulatory element during elongation if dissociated from  $\alpha$ CTD.

#### NusA- $\Delta$ AR2 blocks Rho-dependent termination at $\lambda tR1$ *in vivo*

NusA suppresses termination at certain Rho-dependent sites, e.g. within  $\lambda tR1$  (46). We propose that the NusA:NusG interaction contributes to this effect. To support this hypothesis we asked if a deletion of NusA-AR2 (NusA- $\Delta$ AR2) affected termination at  $\lambda tR1$  *in vivo* (Figure 6). We performed  $\beta$ -galactosidase assays using two fusions to measure termination:  $\lambda cI857 - pR - cro(\Delta RBS) - nutR - tR1 - cII::lacZ$  and  $\lambda cI857 - pR - cro27 - nutR - tR1 - cII::lacZ$ . Termination at  $\lambda tR1$  is indicated by low  $\beta$ -galactosidase activity. Strains carrying a mutation in the *rho* gene show no termination at  $\lambda tR1$ ;  $\beta$ -galactosidase activity of these strains was thus set to 100%. The efficiency of termination at  $\lambda tR1$  was 93% when *cro* translation was prevented by an RBS mutation (strain 10323), and reduced to 74% when *cro* was translated (strain 11149). Ribosomes reduce the amount of free RNA upstream to  $\lambda tR1$  that is available to Rho, and thus block a Rho-binding site (*rut*) in *cro* (47).

We found that termination efficiency was significantly impaired (50%) in the *nusA- $\Delta$ AR2* mutant only when *cro* mRNA was translated (compare strain 10881 to strain 10323 and strain 11699 to strain 11149). Our results suggest that NusA- $\Delta$ AR2 may compete with Rho binding near  $\lambda nutR$ , the only *rut* site available when the *cro* transcript is occluded by ribosomes. When *cro* is not translated, Rho can attach to the free *cro rut* site (48). Competition with Rho by

NusA- $\Delta$ AR2 can be explained by constitutive binding of NusA- $\Delta$ AR2 to RNA *via* NusA-SKK. Consistent with the *in vitro* studies described above, this implies that full length NusA may still be, at least partially, in the autoinhibited state and unable to bind *rut* RNA at  $\lambda tR1$ . It also raises the possibility that NusG may activate RNA binding of full-length NusA by displacing NusA-AR2 from the NusA-SKK domain. Further experimentation will be needed to address these questions.

#### Possible regulatory functions of the NusG-NTD:NusA-AR2 interaction

Transcription factors NusA and NusG act independently to slow or accelerate transcription elongation, respectively. The two factors can also function synergistically in restoring termination by the partially defective RhoE134K mutant (49). Here, however, we demonstrate a direct interaction between NusA and NusG. Formation of a complex between NusG-NTD and NusA-AR2 may explain their various *in vivo* and *in vitro* combinatorial regulatory effects (Figure 7).

##### 1. NusA-AR2 supports NusG recruitment.

NusG:NusA interaction may be involved in recruiting NusG to the TEC. ChIP-chip data suggest that NusA and NusG associate with RNAP when the TEC has exited the promoter region, with NusG attaching after NusA does (50). The delay in NusG association may be due to a competition between  $\sigma^{70}$  region 2 and NusG-NTD, since both bind to the RNAP  $\beta'$ CH (7,51–53). Recall that the  $\sigma^{70}$  region 2 can remain bound to the TEC even when  $\sigma^{70}$  region 4 has dissociated from the  $\beta$  flap, allowing NusA-NTD binding (54,55). After promoter escape, NusA attaches to the  $\alpha$ CTD *via* NusA-AR2, to the  $\beta$  flap *via* NusA-NTD, and to nascent RNA *via* NusA-SKK (10,15,18,56). Thus, stable tethering of NusA to the TEC may not require continuous binding of NusA-AR2 to  $\alpha$ CTD. NusA-AR2 could, therefore, bind NusG-NTD without disrupting the NusA:TEC complex. In this model, NusA serves as a long linker to increase the local concentration of NusG, facilitating NusG recruitment to the TEC and displacement of  $\sigma^{70}$  region 2 from the  $\beta'$ CH at the transition from initiation to elongation.

##### 2. NusG-NTD:NusA-AR2 interaction assists transcription:translation coupling.

As a second function, we suggest that NusG:NusA interaction plays a role in coupling transcription and translation. NusG connects these two processes by physically linking RNAP and the leading ribosome *via* NusG-NTD:RNAP and NusG-CTD:S10 interactions (4,8). The NusA:NusG interaction could serve to resynchronize transcription and translation by coordinating the movements of RNAP and the ribosome. If translation is slowed, transcription could likewise be slowed by the temporary removal of NusG-NTD from the TEC by NusA-AR2. Since the NusG:ribosome connection remains intact, transcription and translation can be kinetically resynchronized. Also, the initial coupling of transcription and translation may occur *via* the NusA:NusG

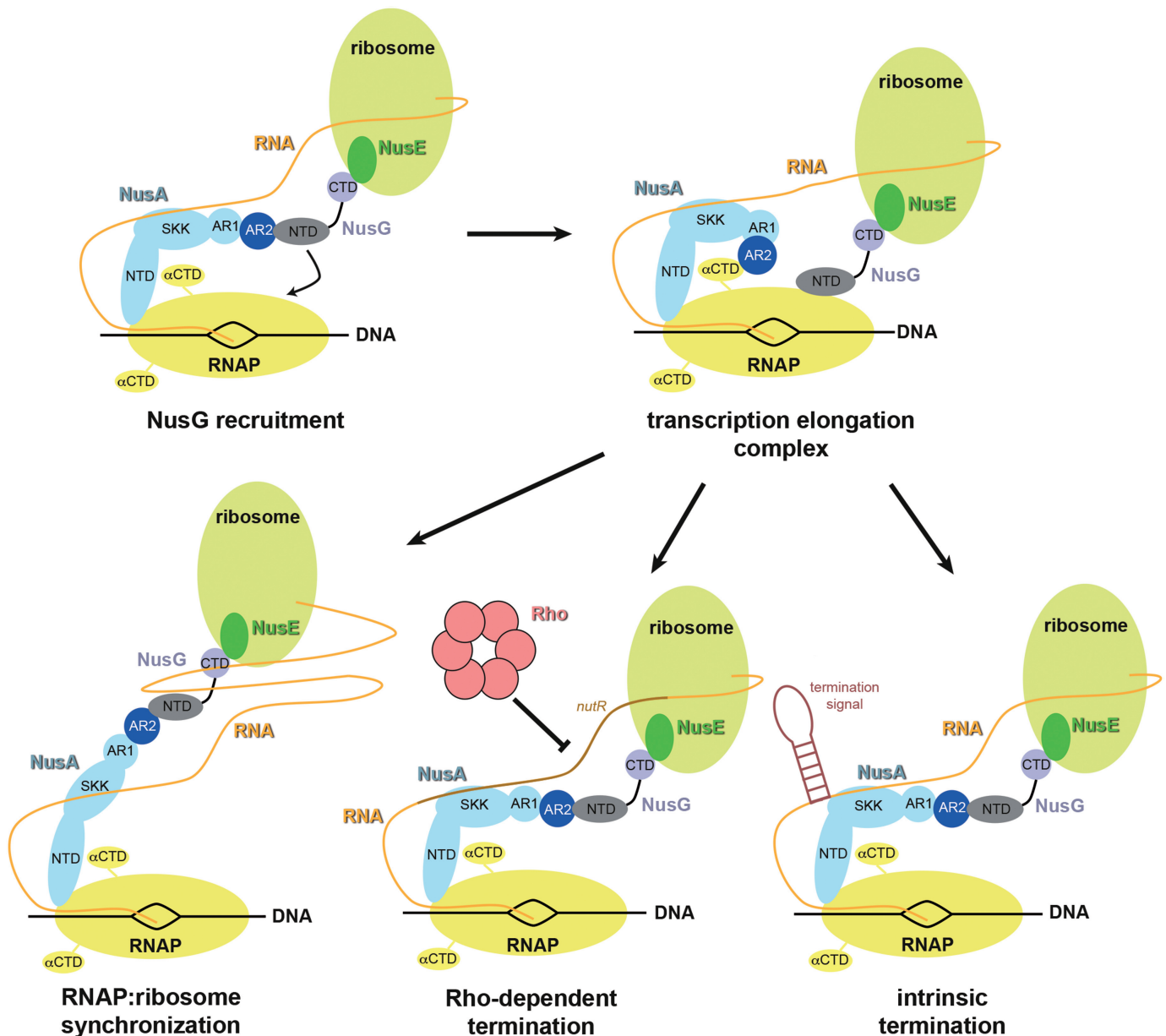


**Figure 7.** Possible functions of NusG:NusA interaction in transcription regulation. First, the NusA:NusG interaction may play a role in the recruitment of NusG to the TEC. Second, it may provide a long linker between RNAP and the ribosome consisting of NusA and NusG, which would allow resynchronization of transcription:translation coupling. Third, the NusG:NusA interaction may release the autoinhibition of NusA allowing constitutive binding of NusA-SKK to RNA, so that recruitment sites for Rho are blocked and Rho-dependent termination is decreased. Forth, NusA-AR2 may abstract NusG-NTD at intrinsic termination sites facilitating the release of nucleic acids and enhancing intrinsic termination.

linker. This would explain the apparent late association of NusG with the TEC, as detected by ChIP-chip experiments (50).

3. NusG-NTD:NusA-AR2 interaction regulates transcription termination.

The NusA:NusG interaction could influence context-dependent intrinsic or Rho-dependent transcription termination. In the former, the TEC pauses at an intrinsic termination signal, enters an elemental pause state, and then isomerizes into the termination state where the termination hairpin is formed (57). NusA-AR2 can remove NusG-NTD from RNAP, resulting in loss of

both NusA-AR2 and NusG-NTD contacts to the TEC (Figure 4E). Loss of these interactions might partially destabilize the TEC, open the clamp around the nucleic acids, and facilitate intrinsic termination. In contrast, the NusA-AR2:NusG-NTD interaction might decrease Rho-dependent termination. Binding of NusA-AR2 to NusG-NTD would release NusA autoinhibition, enhancing binding of NusA-SKK to nascent RNA to block Rho recruitment.

The  $K_D$  values for the various interactions suggest that scenario 1 is the most probable. This scenario is also con-

sistent with a global survey of distribution of transcription factors (50). The relevance of NusG-NTD:NusA-AR2 interaction in detail will need further experimental clarification, but the finding that NusG interacts directly with NusA may explain the various effects of these transcription factors on elongation and termination reported here and earlier.

## SUPPLEMENTARY DATA

Supplementary Data are available at NAR Online.

## ACKNOWLEDGEMENTS

M.S., S.H.K., P.R. thank Ramona Heißmann for excellent technical support. We also thank Dr J. Drögemüller for carefully reading the manuscript and Drs J. Drögemüller and R. Washburn for helpful discussions.

## FUNDING

Deutsche Forschungsgemeinschaft [Ro 617/21-1 to P.R.]; Ludwig-Schaefer-Scholarship 2015 from the Columbia University Medical Center (to P.R.); National Institutes of Health [GM37219 to M.G.]. Funding for open access charge: Universität Bayreuth.

Conflict of interest statement. None declared.

## REFERENCES

- Werner, F. and Grohmann, D. (2011) Evolution of multisubunit RNA polymerases in the three domains of life. *Nat. Rev. Microbiol.*, **9**, 85–98.
- Mooney, R.A., Artsimovitch, I. and Landick, R. (1998) Information processing by RNA polymerase: recognition of regulatory signals during RNA chain elongation. *J. Bacteriol.*, **180**, 3265–3275.
- Burns, C.M., Richardson, L.V. and Richardson, J.P. (1998) Combinatorial effects of NusA and NusG on transcription elongation and rho-dependent termination in *Escherichia coli*. *J. Mol. Biol.*, **278**, 307–316.
- Mooney, R.A., Schweimer, K., Rösch, P., Gottesman, M.E. and Landick, R. (2009) Two structurally independent domains of *E. coli* NusG create regulatory plasticity via distinct interactions with RNA polymerase and regulators. *J. Mol. Biol.*, **391**, 341–358.
- Werner, F. (2012) A nexus for gene expression-molecular mechanisms of Spt5 and NusG in the three domains of life. *J. Mol. Biol.*, **417**, 13–27.
- Sevostyanova, A., Belogurov, G.A., Mooney, R.A., Landick, R. and Artsimovitch, I. (2011) The  $\beta$  subunit gate loop is required for RNA polymerase modification by RfaH and NusG. *Mol. Cell*, **43**, 253–262.
- Martinez-Rucobo, F.W., Sainsbury, S., Cheung, A.C. and Cramer, P. (2011) Architecture of the RNA polymerase-Spt4/5 complex and basis of universal transcription processivity. *EMBO J.*, **30**, 1302–1310.
- Burmam, B.M., Schweimer, K., Luo, X., Wahl, M.C., Stitt, B.L., Gottesman, M.E. and Rösch, P. (2010) A NusE:NusG complex links transcription and translation. *Science*, **328**, 501–504.
- Friedman, D.I., Schauer, A.T., Baumann, M.R., Baron, L.S. and Adhya, S.L. (1981) Evidence that ribosomal protein S10 participates in control of transcription termination. *Proc. Natl. Acad. Sci. U.S.A.*, **78**, 1115–1118.
- Yang, X., Molimau, S., Doherty, G.P., Johnston, E.B., Marles-Wright, J., Rothnagel, R., Hankamer, B., Lewis, R.J. and Lewis, P.J. (2009) The structure of bacterial RNA polymerase in complex with the essential transcription elongation factor NusA. *EMBO Rep.*, **10**, 997–1002.
- Ha, K.S., Toulkhonov, I., Vassilyev, D.G. and Landick, R. (2010) The NusA N-terminal domain is necessary and sufficient for enhancement of transcriptional pausing via interaction with the RNA exit channel of RNA polymerase. *J. Mol. Biol.*, **401**, 708–725.
- Ma, C., Mobli, M., Yang, X., Keller, A.N., King, G.F. and Lewis, P.J. (2015) RNA polymerase-induced remodelling of NusA produces a pause enhancement complex. *Nucl. Acids Res.*, **43**, 2829–2840.
- Eisenmann, A., Schwarz, S., Prasch, S., Schweimer, K. and Rösch, P. (2005) The *E. coli* NusA carboxy-terminal domains are structurally similar and show specific RNAP- and  $\lambda$ N interaction. *Protein Sci.*, **14**, 2018–2029.
- Worbs, M., Bourenkov, G.P., Bartunik, H.D., Huber, R. and Wahl, M.C. (2001) An extended RNA binding surface through arrayed S1 and KH domains in transcription factor NusA. *Mol. Cell*, **7**, 1177–1189.
- Mah, T.F., Li, J., Davidson, A.R. and Greenblatt, J. (1999) Functional importance of regions in *Escherichia coli* elongation factor NusA that interact with RNA polymerase, the bacteriophage lambda N protein and RNA. *Mol. Microbiol.*, **34**, 523–537.
- Prasch, S., Schwarz, S., Eisenmann, A., Wöhr, B.M., Schweimer, K. and Rösch, P. (2006) Interaction of the intrinsically unstructured phage lambda N protein with *E. coli* NusA. *Biochemistry*, **45**, 4542–4549.
- Mishra, S., Mohan, S., Godavarthi, S. and Sen, R. (2013) The interaction surface of a bacterial transcription elongation factor required for complex formation with an antiterminator during transcription antitermination. *J. Biol. Chem.*, **288**, 28089–28103.
- Schweimer, K., Prasch, S., Santhanam, S.P., Bubunenko, M., Gottesman, M.E. and Rösch, P. (2011) NusA interaction with the  $\alpha$ -subunit of *E. coli* RNA polymerase is via the UP-element site and releases autoinhibition. *Structure*, **19**, 945–954.
- Artsimovitch, I. and Landick, R. (2000) Pausing by bacterial RNA polymerase is mediated by mechanically distinct classes of signals. *Proc. Natl. Acad. Sci. U.S.A.*, **97**, 7090–7095.
- Cardinale, C.J., Washburn, R.S., Tadigotla, V.R., Brown, L.M., Gottesman, M.E. and Nudler, E. (2008) Termination factor Rho and its cofactors NusA and NusG silence foreign DNA in *E. coli*. *Science*, **320**, 935–938.
- Mason, S.W., Li, J. and Greenblatt, J. (1992) Host factor requirements for processive antitermination of transcription and suppression of pausing by the N protein of bacteriophage lambda. *J. Biol. Chem.*, **267**, 19418–19426.
- Shankar, S., Hatoum, A. and Roberts, J.W. (2007) A transcription antiterminator constructs a NusA-dependent shield to the emerging transcript. *Mol. Cell*, **27**, 914–927.
- Weisberg, R.A. and Gottesman, M.E. (1999) Processive antitermination. *J. Bacteriol.*, **181**, 359–367.
- Borukhov, S., Lee, J. and Laptenko, O. (2005) Bacterial transcription elongation factors: New insights into molecular mechanism of action. *Mol. Microbiol.*, **55**, 1315–1324.
- Roberts, J.W., Shankar, S. and Filter, J.J. (2008) RNA polymerase elongation factors. *Annu. Rev. Microbiol.*, **62**, 211–233.
- Li, J., Mason, S.W. and Greenblatt, J. (1993) Elongation factor NusG interacts with termination factor Rho to regulate termination and antitermination of transcription. *Genes Dev.*, **7**, 161–172.
- Nehrke, K.W., Zalatan, F. and Platt, T. (1993) NusG alters Rho-dependent termination of transcription *in vitro* independent of kinetic coupling. *Gene Expr.*, **3**, 119–133.
- Kohno, T., Kusunoki, H., Sato, K. and Wakamatsu, K. (1998) A new general method for the biosynthesis of stable isotope-enriched peptides using a decahistidine-tagged ubiquitin fusion system: An application to the production of mastoparan-X uniformly enriched with  $^{15}\text{N}$  and  $^{15}\text{N}/^{13}\text{C}$ . *J. Biomol. NMR*, **12**, 109–121.
- Burmam, B.M., Schweimer, K., Scheckenhofer, U. and Rösch, P. (2011) Domain interactions of the transcription: Translation coupling factor *E. coli* NusG are intermolecular and transient. *Biochem. J.*, **435**, 783–789.
- Drögemüller, J., Strauss, M., Schweimer, K., Wöhr, B.M., Knauer, S.H. and Rösch, P. (2015) Exploring RNA polymerase regulation by NMR spectroscopy. *Sci. Rep.*, **5**, 10825–10835.
- Prasch, S., Jurk, M., Washburn, R.S., Gottesman, M.E., Wöhr, B.M. and Rösch, P. (2009) RNA-binding specificity of *E. coli* NusA. *Nucleic Acids Res.*, **37**, 4736–4742.
- Eisenmann, A., Schwarz, S., Prasch, S., Schweimer, K. and Rosch, P. (2005) The *E. coli* NusA carboxy-terminal domains are structurally similar and show specific RNAP- and lambdaN interaction. *Protein Sci.*, **14**, 2018–2029.

33. Eisenmann, A., Schwarz, S., Rösch, P. and Schweimer, K. (2004) Sequence-specific  $^1\text{H}$ ,  $^{13}\text{C}$ ,  $^{15}\text{N}$  resonance assignments and secondary structure of the carboxyterminal domain of the *E. coli* transcription factor NusA. *J. Biomol. NMR*, **28**, 193–194.
34. Artsimovitch, I., Svetlov, V., Murakami, K.S. and Landick, R. (2003) Co-overexpression of *Escherichia coli* RNA polymerase subunits allows isolation and analysis of mutant enzymes lacking lineage-specific sequence insertions. *J. Biol. Chem.*, **278**, 12344–12355.
35. Kashlev, M., Martin, E., Polyakov, A., Severinov, K., Nikiforov, V. and Goldfarb, A. (1993) Histidine-tagged RNA polymerase: Dissection of the transcription cycle using immobilized enzyme. *Gene*, **130**, 9–14.
36. Sambrook, J., Fritsch, E.F. and Maniatis, T. (1994) *Molecular Cloning – A Laboratory Manual*. Cold Spring Harbor Laboratory Press, NY.
37. Meyer, O. and Schlegel, H.G. (1983) Biology of aerobic carbon monoxide-oxidizing bacteria. *Annu. Rev. Microbiol.*, **37**, 277–310.
38. Vitiello, C.L., Kireeva, M.L., Lubkowska, L., Kashlev, M. and Gottesman, M. (2014) Coliphage HK022 nun protein inhibits RNA polymerase translocation. *Proc. Natl. Acad. Sci. U.S.A.*, **111**, E2368–E2375.
39. Johnson, B.A. (2004) Using NMRView to visualize and analyze the NMR spectra of macromolecules. *Methods Mol. Biol.*, **278**, 313–352.
40. de Vries, S.J., van Dijk, M. and Bonvin, A.M. (2010) The HADDOCK web server for data-driven biomolecular docking. *Nat. Protoc.*, **5**, 883–897.
41. Posfai, G., Plunkett, G. 3rd, Feher, T., Frisch, D., Keil, G.M., Umenhoffer, K., Kolisnychenko, V., Stahl, B., Sharma, S.S., de Arruda, M. *et al.* (2006) Emergent properties of reduced-genome *Escherichia coli*. *Science*, **312**, 1044–1046.
42. Svenningsen, S.L., Costantino, N., Court, D.L. and Adhya, S. (2005) On the role of Cro in lambda prophage induction. *Proc. Natl. Acad. Sci. U.S.A.*, **102**, 4465–4469.
43. Schrödinger, L. (2010) *The PyMOL Molecular Graphics System, version 1.3*. Schrödinger, LLC, Mannheim.
44. Sievers, F., Wilm, A., Dineen, D., Gibson, T.J., Karplus, K., Li, W., Lopez, R., McWilliam, H., Remmert, M., Soding, J. *et al.* (2011) Fast, scalable generation of high-quality protein multiple sequence alignments using clustal omega. *Mol. Syst. Biol.*, **7**, 539.
45. Drögemüller, J., Strauß, M., Schweimer, K., Jurk, M., Rösch, P. and Knauer, S.H. (2015) Determination of RNA polymerase binding surfaces of transcription factors by NMR spectroscopy. *Sci. Rep.*, **5**, 16428–16441.
46. Lau, L.F., Roberts, J.W. and Wu, R. (1983) RNA polymerase pausing and transcript release at the lambda *tR1* terminator *in vitro*. *J. Biol. Chem.*, **258**, 9391–9397.
47. Faus, I. and Richardson, J.P. (1990) Structural and functional properties of the segments of lambda *cro* mRNA that interact with transcription termination factor Rho. *J. Mol. Biol.*, **212**, 53–66.
48. Graham, J.E. and Richardson, J.P. (1998) *Rut* sites in the nascent transcript mediate Rho-dependent transcription termination *in vivo*. *J. Biol. Chem.*, **273**, 20764–20769.
49. Muteeb, G., Dey, D., Mishra, S. and Sen, R. (2012) A multipronged strategy of an anti-terminator protein to overcome Rho-dependent transcription termination. *Nucleic Acids Res.*, **40**, 11213–11228.
50. Mooney, R.A., Davis, S.E., Peters, J.M., Rowland, J.L., Ansari, A.Z. and Landick, R. (2009) Regulator trafficking on bacterial transcription units *in vivo*. *Mol. Cell*, **33**, 97–108.
51. Belogurov, G.A., Vassilyeva, M.N., Svetlov, V., Klyuyev, S., Grishin, N.V., Vassilyev, D.G. and Artsimovitch, I. (2007) Structural basis for converting a general transcription factor into an operon-specific virulence regulator. *Mol. Cell*, **26**, 117–129.
52. Arthur, T.M. and Burgess, R.R. (1998) Localization of a sigma70 binding site on the N terminus of the *Escherichia coli* RNA polymerase beta' subunit. *J. Biol. Chem.*, **273**, 31381–31387.
53. Young, B.A., Anthony, L.C., Gruber, T.M., Arthur, T.M., Heyduk, E., Lu, C.Z., Sharp, M.M., Heyduk, T., Burgess, R.R. and Gross, C.A. (2001) A coiled-coil from the RNA polymerase beta' subunit allosterically induces selective nontemplate strand binding by sigma(70). *Cell*, **105**, 935–944.
54. Bar-Nahum, G. and Nudler, E. (2001) Isolation and characterization of sigma(70)-retaining transcription elongation complexes from *Escherichia coli*. *Cell*, **106**, 443–451.
55. Kuznedelov, K., Minakhin, L., Niedziela-Majka, A., Dove, S.L., Rogulja, D., Nickels, B.E., Hochschild, A., Heyduk, T. and Severinov, K. (2002) A role for interaction of the RNA polymerase flap domain with the sigma subunit in promoter recognition. *Science*, **295**, 855–857.
56. Mah, T.F., Kuznedelov, K., Mushegian, A., Severinov, K. and Greenblatt, J. (2000) The alpha subunit of *E. coli* RNA polymerase activates RNA binding by NusA. *Genes Dev.*, **14**, 2664–2675.
57. Weixlbaumer, A., Leon, K., Landick, R. and Darst, S.A. (2013) Structural basis of transcriptional pausing in bacteria. *Cell*, **152**, 431–441.